Volume 10, Issue 1, 2020, 4734 - 4739 ISSN 2069-5837
Biointerface Research in Applied Chemistry
www.BiointerfaceResearch.com
https://doi.org/10.33263/BRIAC101.734739
Original Research Article Open Access Journal
Received: 23.09.2019 / Revised: 11.11.2019 / Accepted: 17.11.2019 / Published on-line: 21.11.2019

# Molecular properties of polyvinyl alcohol/ sodium alginate composite

**Ahmed Fahmy [1], Rasha M. Khafagy [2], Hanan Elhaes [2], Medhat A. Ibrahim [1,*]**
[1]Spectroscopy Department, National Research Centre, 33 El-Bohouth St., 12622 Dokki, Giza, Egypt
[2]Physics Department, Faculty of Women for Arts, Science and Education, Ain Shams University, 11757, Cairo, Egypt
*corresponding author e-mail address: ***medahmed6@yahoo.com*** | Scopus ID 8641587100

## ABSTRACT
Molecular and bimolecular properties are important factors to judge the functionality of polymer/biopolymer composites. Accordingly, molecular modeling is conducted to study the electronic properties of Polyvinyl Alcohol (PVA); Sodium Alginate (SA) as well as their composites. Accordingly, Density functional theory (DFT) at B3LYB level using 6-311/G (d, p) basis set is utilized to study the model structures. Total dipole moment (TDM), HOMO/LUMO energy gap, electrostatic potential (ESP) are calculated at B3LYB level for all studied structures. The results of TDM, HOMO/LUMO energy gap and ESP indicated that the TDM increased, HOMO/LUMO energy gap decreased and electro-negativity increased for the structures under study. Thermal parameters at PM6 are calculated including final heat of formation; free energy; entropy; enthalpy and heat capacity as a function of temperature. Thermal parameters show a variation with changing the site of interaction which indicated that the coordination of PVA/SA is an important factor for describing PVA/SA composite.
**Keywords:** *PVA; SA; DFT; TDM and HOMO/LUMO band gap energy.*

## 1. INTRODUCTION
Sodium alginate is a linear biopolymers belonging to polysaccharide family its chemical structure is ($NaC_6H_7O_6$) and termed SA [1]. It is also described as derivative of alginic acid comprised of 1,4-β-d-mannuronic (M) and α-l-guluronic (G) acids, its molecular structure show many carboxyl groups [2-3]. SA has common features dedicates it for different applications. It is abundant, water-soluble, renewable, and nontoxic, accordingly it is also biodegradable and biocompatible. Although it is biological candidate for its important features, SA is also mechanically poor, which in turn allows bacteria to degrade it especially in waste water and extreme environmental conditions [4-7].

SA could be subjected to modification chemically or physically to improve its physicochemical properties and subsequently its biological activity. The modified SA is forming so called SA derivatives, which are dedicating for different types of application based on the type of modifications. [8-9]. Meanwhile, polyvinyl alcohol is made from the hydrolysis of polyvinyl acetate, it is termed as PVA, and it is water soluble [10]. In the last century it is worldwide applied in several industrial applications [11]. Rather than natural polymers, synthetic polymers such as PVA are non-renewable and non-biodegradable sources [12], but it is non toxic. These properties dedicate PVA as thermoplastic polymer, widely use in cross-linked products and nanofillers. Based on these properties, PVA could gain further properties when it is blended with biopolymers [13-15].

This paves the way toward unique molecular, biomolecular and electronic properties of blended synthetic and biopolymers. So that, modifying the chemical and physical characteristics of biopolymers such as SA requires the addition of agent controlling its properties such as PVA.

Molecular modeling with different level of theories could be tools of concern to study electronic properties of synthetic and/or biopolymers [16-19]. Investigating electronic properties of such composites is an important step toward understanding the functionality of polymers for advanced applications [20-21].
It is stated that molecular modeling as an effective tool to elucidate the molecular and biomolecular properties of many systems and molecules to confirm, fulfill and/or assign the experimental results [22-28].

Based upon the above considerations the present work is conducted to model the electronic properties of PVA; and their composite at DFT and PM6 semi-empirical computational levels.

## 2. MATERIALS AND METHODS
### 2.1. Calculation details.
Model molecules representing PVA, SA and PVA/SA composite are built up. Models are subjected to calculation using Gaussian 09 software [29] at Spectroscopy Department, National Research Centre, Egypt. Models are optimized with Density functional theory (DFT) at B3LYP level [30-32], with 6-311g (d, p) basis set. Physical quantities such as total dipole moment, HOMO/LUMO band gap energy and electrostatic potential (ESP) are computed at the same quantum mechanical level. The same structures are optimized at PM6 then final heat of formation; free energy; entropy; enthalpy and heat capacity are calculated with SCIGRESS [33] soft code at Spectroscopy Department, National Research Centre, Egypt.

## 3. RESULTS
**3.1. Building model molecules.** Studying the electronic properties of PVA and SA was done through a number of stages. The first stage is the creation of the model molecules which represent PVA, SAand PVA interacted with SA. Three units of PVA (3 PVA or trimer PVA) and two of SA (2 SA or dimer SA) are considered in the present work. Figure 1 shows the supposed structures of PVA

and SA. The interaction between the functional groups of PVA and that of SA is supposed to be weak interaction. However, there are two possible ways of interaction. PVA in its trimer form contains three hydroxyl groups. Then SA can interact with PVA at the different positions of OH group. So that, the first way of interaction, is that each unit of dimer SA can interact with PVA separately at different positions. While, the second way is that, the model molecule representing dimer SA, as a bulk, is interacted with PVA throughout the hydroxyl groups of PVA which, are connected to carbon atom number 5, 10 and 21 respectively as presented in figure 2. All studied structures are subjected to single point energy calculations.

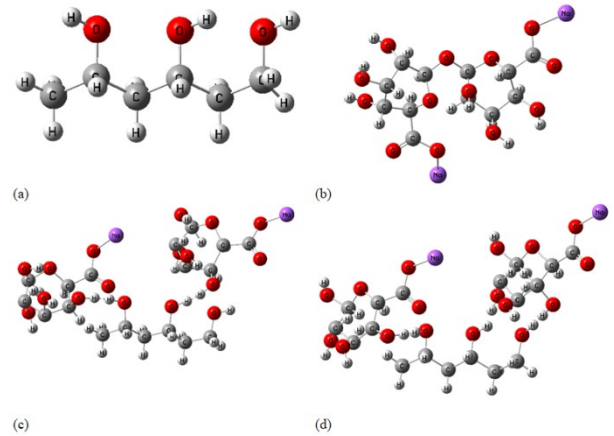

**Figure 1.** Model molecules representing a) 3 PVA; b) 2 SA; c) 3PVA- Term 1SA -Term 1SA and d) 3PVA- Term 1SA -Mid 1Na.

### 3.2. TDM and HOMO/LUMO band gap energy.

Based on the literature, the change in electronic properties of polymeric materials can be studied in terms of total dipole moment (TDM) and HOMO/LUMO band gap energy as they can predict the stability and reactivity of the molecular structures [34]. TDM as Debye and HOMO/LUMO band gap energy ΔE as eV are calculated at B3LYP/6-311g (d, p).

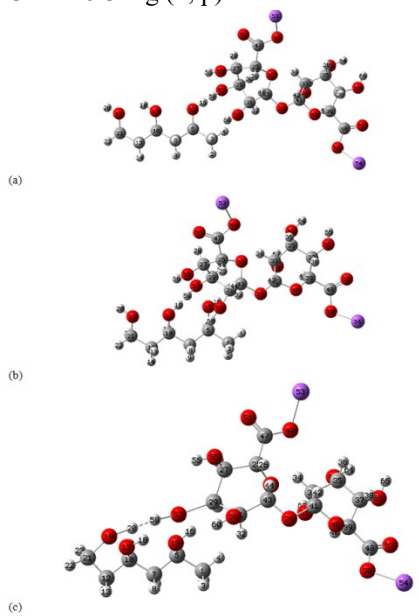

**Figure 2.** Model molecules represented a) 3PVA- ($C_5$) 2SA; b) 3PVA- ($C_{10}$) 2SA and c) 3PVA- ($C_{21}$) 2SA.

As depicted in table 1 that trimer PVA (3PVA) and dimer SA (2 SA) possess a TDM of 4.2172 and 9.2543 Debye respectively. However, the calculated HOMO/LUMO band gap energies of 3PVA and 2 SAare 7.4478 and 2.5293eV respectively. As a result of adding 2SAto the proposed structure of PVA, it was observed that both TDM and HOMO/LUMO band gap energies of trimer PVA and dimer SA suffers strong changes in their values. Where, for the first way of interaction, the TDM was increased to 20.6941 and 24.6199 Debye for Term 1SA -3PVA- Term 1SA and Term 1SA - 3PVA- Mid. 1SA respectively. However, HOMO/LUMO band gap energy was decreased to 0.9559 and 0.5706eV for the same sequence. The distribution of HOMO/LUMO band gap energies were presented in figure 3 for 3PVA, 2SA, Term 1SA -3PVA- Term 1SA and Term 1SA-3PVA- Mid 1SA.

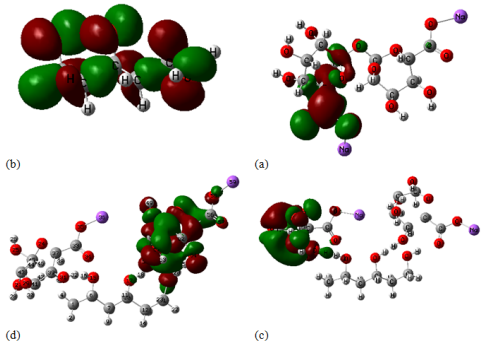

**Figure 3.** HOMO/LUMO band gap energy calculated at B3LYP/(6-311) G (d, p) for: a) 3 PVA; b) 2 SA; c) 3PVA- Term 1SA -Term 1SA and d) 3PVA- Term 1SA -Mid 1Na.

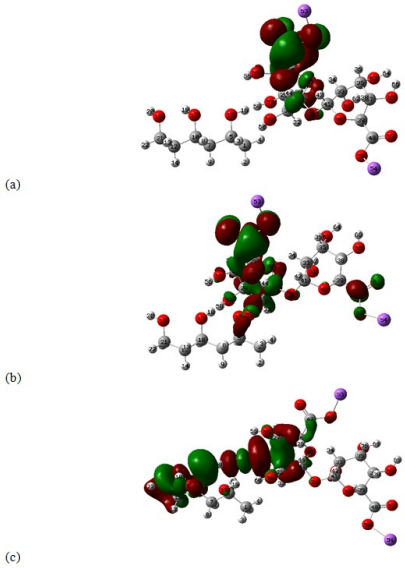

**Figure 4.** HOMO/LUMO band gap energy calculated at B3LYP/(6-311) G (d,p) for: a) 3PVA- ($C_5$) 2SA; b) 3PVA- ($C_{10}$) 2SA and c) 3PVA- ($C_{21}$) 2SA.

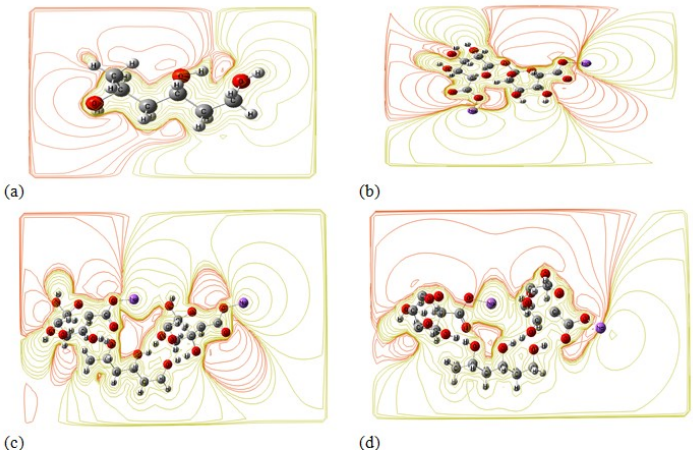

**Figure 5.** Calculated ESP at B3LYP/(6-311) G (d,p) as contour action for: a) 3 PVA; b) 2 SA; c) 3PVA- Term 1SA -Term 1SA and d) 3PVA- Term 1SA -Mid 1Na.

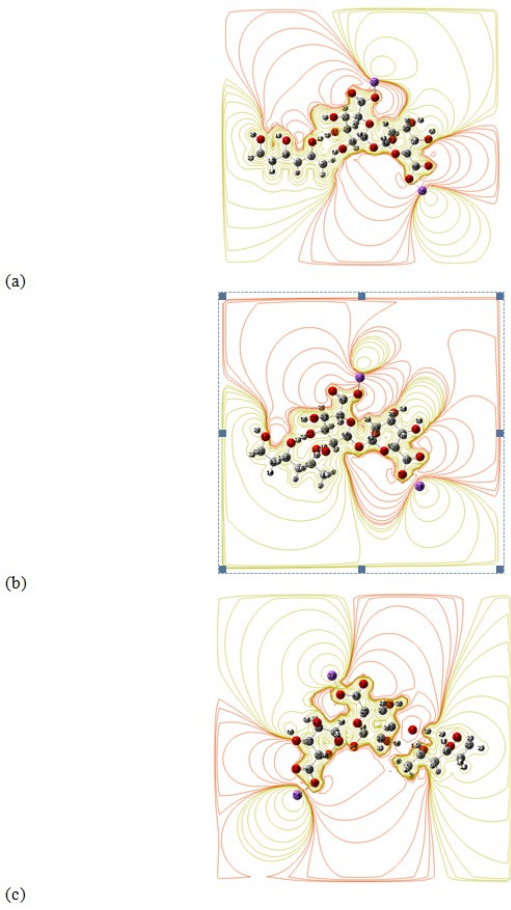


**Figure 6.** Calculated ESP at B3LYP/ (6-311) G (d, p) as contour action for: a) 3PVA- ($C_5$) 2SA; b) 3PVA- ($C_{10}$) 2SA and c) 3PVA- ($C_{21}$) 2SA.

On the other hand, for the second possibility of interaction as presented in table 2, TDM increased slightly to 8.0586, 12.2080 and 7.2146 Debye for 3PVA- (C5) 2SA, 3PVA- (C10) 2SA and 3PVA- (C21) 2SArespectively. Meanwhile, HOMO/LUMO band gap energy was changed to 2.9772, 0.2908 and 2.1511 eV (see table 2) for 3PVA- ($C_5$) 2SA, 3PVA- ($C_{10}$) 2SA and 3PVA- ($C_{21}$) 2SA respectively. Figure 4 shows the calculated band gap energy for 3PVA- ($C_5$) 2SA, 3PVA- ($C_{10}$) 2SA and 3PVA- ($C_{21}$) 2SA respectively.

### 3.3. Electrostatic potential (ESP).

Electrostatic potentials (ESPs) are calculated also for all structures at B3LYP/ (6-311) G (d, p) level. The reactivity of polymeric materials can be estimated by studying their ESP. Figures 5 and 6 present the calculated ESPs for all model molecules as contour action. It is stated that, the reactivity of molecular structures can be studied by following a color map ranging from high to low values as follow: red > orange > yellow > green > blue. This sequence of colors refers to the distribution of charges within the structures. The red color, which is distributed around the molecules, refers to that electro-negativity is high and also the reactivity of those molecules increased. However, the neutral charges and positive ones can be noticed with yellow and blue colors respectively [35-37]. So, as shown in the figures, that the PVA reactivity was increased by interaction with SA.

The changes of the values of TDM and that of HOMO/LUMO band gaps, together with ESP results, refers to the strong interaction that takes place between the proposed structures of PVA and SA. This can be attributed to the presence of hydroxyl groups in PVA and SA structures.

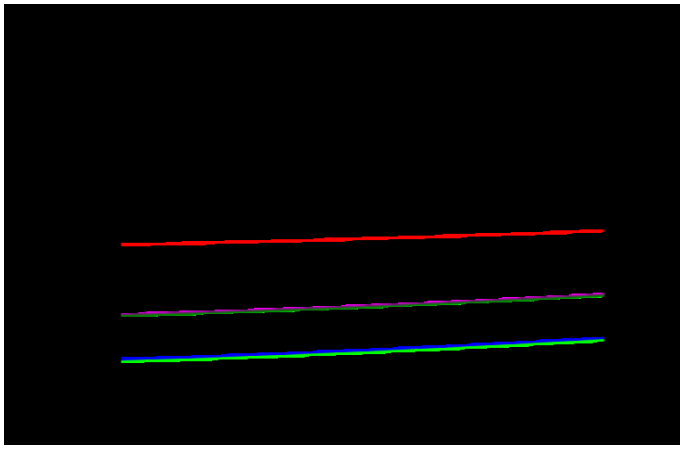

**Figure 7**. Heat of formation as a function of temperature for a) 3 PVA, b) 2 SA c) term SA- 3PVA- mid SA d) term SA- 3 PVA- term SA e) 3 PVA - 2 SA - C5 f) 3 PVA - 2 SA - C10 and g) 3 PVA -2 SA -C21 calculated at PM6 level of theory.

### 3.4. Calculated thermal parameters.

Thermal parameters of polymeric materials and their composites are very important in order to know their possible applications and functionality. In this work there are different ways of composite interaction sites so that some parameters will be calculated.

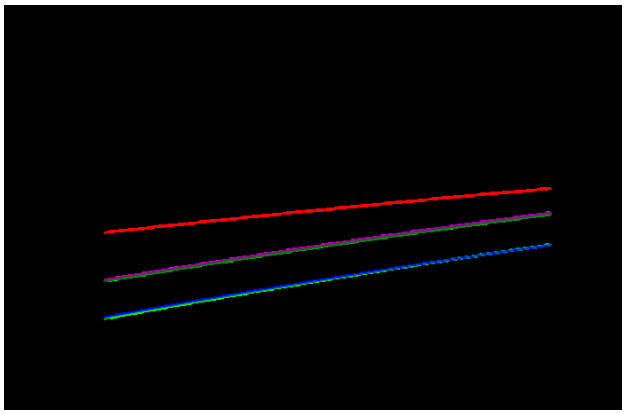

**Figure 8.** Free energy as a function of temperature for a) 3 PVA, b) 2 SA c) term SA- 3PVA- mid SA d) term SA- 3 PVA- term SA e) 3 PVA - 2 SA - C5 f) 3 PVA - 2 SA - C10 and g) 3 PVA -2 SA -C21 calculated at PM6 level of theory.

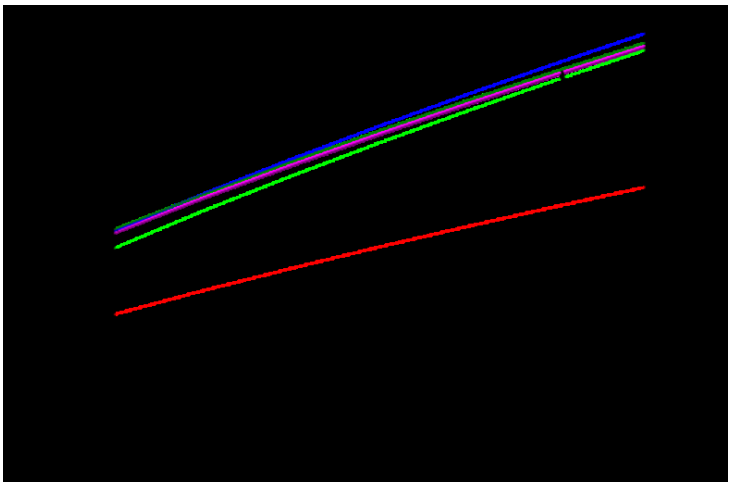

**Figure 9**. Entropy as a function of temperature for a) 3 PVA, b) 2 SA c) term SA- 3PVA- mid SA d) term SA- 3 PVA- term SA e) 3 PVA - 2 SA - C5 f) 3 PVA - 2 SA - C10 and g) 3 PVA -2 SA -C21 calculated at PM6 level of theory.

PM6 semi-empirical quantum mechanical method is utilized to calculate thermal parameters namely final heat of formation; free energy; entropy; enthalpy and heat capacity. These thermal terms could be defined simply as in the following [27-28]. The heat of formation is the amount of heat released or absorbed during the formation of certain pure substance from its constituents elements at constant pressure. Free energy could be defined as the energy-like property it is meaning that its magnitude depends on the amount of a substance in a given thermodynamic state.

Entropy is the measure of a system's thermal energy per unit temperature that is unavailable for doing useful work. Because work is obtained from ordered molecular motion, the amount of entropy is also a measure of the molecular disorder, or randomness, of a system. When certain substance changes at constant pressure, Enthalpy tells how much heat and work were added or removed from this substance. Finally, the heat capacity is defined as the amount of heat required to change temperature of the substance by one degree. The studied thermal parameters as function of temperature in the range of 200 to 500 k are described as indicated in figures 7 to 11.

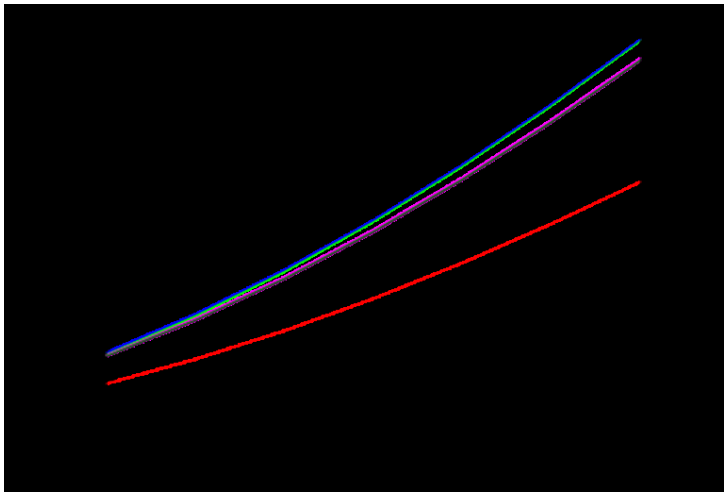

**Figure 10**. Enthalpy as a function of temperature for a) 3 PVA, b) 2 SA c) term SA- 3PVA- mid SA d) term SA- 3 PVA- term SA e) 3 PVA - 2 SA - C5 f) 3 PVA - 2 SA - C10 and g) 3 PVA -2 SA -C21 calculated at PM6 level of theory.

Figure 7 presents the PM6 calculated heat of formation as a function of temperature for the studied structures. It is clear from the figure that the heat of formation has a linear dependence of temperature and increases with increasing the temperature. Also, the figure indicated that the studied structures representing trimmer PVA possess the highest amount of heat of formation in comparison with dimer SA and the interacted 3PVA. Moreover, the figure indicated that the interactions which proceed through the OH group attached to carbon atom number 5, 10 and 21 have nearly the same heat of formation. Similarly, the interaction of each unit of dimer SA with 3PVA at different positions also needs the same quantity of heat of formation. Finally, it was concluded that the heat of formation follow in its values, from highest to the lowest values, the following sequence: 3 PVA> 2 SA >3 PVA- 2 SA - (C5 = C10 = C21)> (term SA - 3 PVA- termSA= term SA- 3PVA- mid SA).

Figure 8 shows the variation of free energy for all studied structures as K Cal/Mol with temperature as K. The figure indicated that the free energy increased with increasing temperature for all the studied structures and that 3PVA possesses the highest values of free energy. Also, like the heat of formation, the free energy following the same sequence as 3 PVA> 2 SA> 3 PVA- 2 SA- (C5 = C10 = C21)> (term SA- 3 PVA- term SA = term SA- 3PVA- mid SA) in its values.

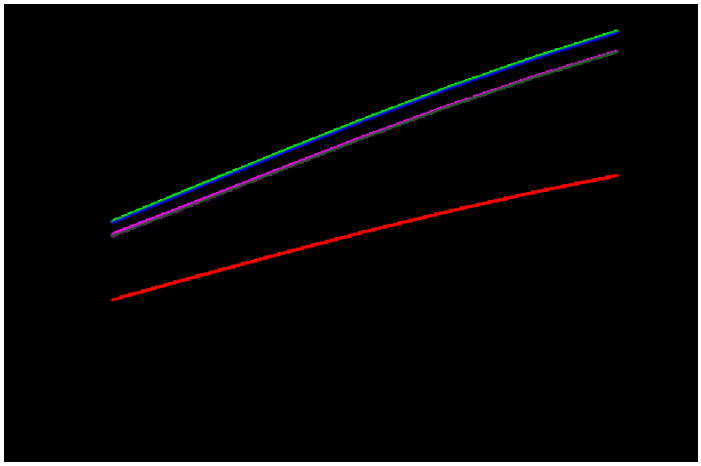

**Figure 11**. Heat capacity as a function of temperature for a) 3 PVA, b) 2 SA c) term SA- 3PVA- mid SA d) term SA- 3 PVA- term SA e) 3 PVA - 2 SA - C5 f) 3 PVA - 2 SA - C10 and g) 3 PVA -2 SA -C21 calculated at PM6 level of theory.

**Table 1.** B3LYP/6-311G (d,p) computed total dipole moment (TDM) as Debye; HOMO-LUMO band gap energies (ΔE) as eV for 3 PVA; 2 SA; 3PVA- Term 1SA -Term 1SA and 3PVA- Term 1SA -Mid 1Na.

| Structure | TDM | ΔE |
|---|---|---|
| 3PVA | 4.2172 | 7.4478 |
| 2 SA | 9.2543 | 2.5293 |
| Term 1SA - 3PVA- Term 1SA | 20.6941 | 0.9559 |
| Term 1SA - 3PVA- Mid. 1SA | 24.6199 | 0.5706 |

**Table 2.** B3LYP/6-311G (d,p) computed total dipole moment (TDM) as Debye; HOMO-LUMO band gap energies (ΔE) as eV for 3PVA- ($C_5$) 2SA; 3PVA- ($C_{10}$) 2SA and 3PVA- ($C_{21}$) 2SA.

| Structure | TDM | ΔE |
|---|---|---|
| 3PVA- ($C_5$) 2SA | 8.0586 | 2.9772 |
| 3PVA- ($C_{10}$) 2SA | 12.2080 | 0.2908 |
| 3PVA- ($C_{21}$) 2SA | 7.2146 | 2.1511 |

Moreover, the entropy as Cal/K/Mole was also calculated for the proposed structures of trimmer PVA, dimer SA, term 1SA- 3PVA- term 1SA, term 1SA- 3PVA- mid 1SA, 3PVA- (C5) 2 SA, 3PVA- (C10) 2 SA and 3PVA- (C21) 2 SA. The variation of entropy was presented in figure 9 as a function of temperature. The figure indicated that the entropy was increased with increasing temperature from 200K to 500K and that the relationship between entropy and temperature was linear for the studied structures. As shown in the figure, the entropy of dimer SA is higher than that of 3PVA. Also, as a result of interaction with SA, the entropy of 3PVA was changed and rise to higher values. Where the entropy of 3PVA interacted with the two units of dimer SA at the two terminal OH groups of 3PVA is the highest one compared to other structures. Here, entropy of Term 1SA - 3PVA- Mid. 1SA is lower than that of Term 1SA - 3PVA- Term. 1SA. However, for the second probability of interaction of 3PVA with 2 SA, there are no considerable changes between the entropy of the blended structures as a result of changing the OH group position. Where, the three curves for 3 PVA> 2 SA> 3 PVA- 2 SA- (C5 = C10 = C21) are nearly close to each other. All these

results of heat of formation, free energy and entropy agree with the results of calculated TDM, HOMO/LUMO band gap and ESP. Additionally, figure 10 and figure 11 represents the variation of both enthalpy as (Cal/Mole) and the heat capacity as (Cal/Mole/K) with temperature for all the studied structures. The same behavior of entropy was observed in figures 10 and 11 for enthalpy and heat capacity. Where the highest values of both quantities belong to the model molecule representing Term 1SA - 3PVA- Mid. 1SA and Term 1SA - 3PVA- Term 1SA.

The overall thermal parameters show a variation in its studied values as the site of interaction is changing so that the coordination of PVA/SA is an important factor for describing PVA/SA composite

## 4. CONCLUSIONS

Studying the electronic properties of PVA and SA based on DFT principals was carried out. The total dipole moment, HOMO/LUMO band gap energy and electrostatic potential were studied. As a result of the interaction of PVA with SA, it was found that generally, TDM of PVA and that of SA was increased. Where, for the first probability of interaction, TDM was increased to 24.6199 Debye. Meanwhile, the band gap energy was decreased to 0.5706eV as a result of interaction. However, for the second probability of interaction, the highest TDM was 12.2080 Debye for the dimer SA interacted with trimer PVA throughout the middle OH group. In contrast, the lowest value of HOMO/LUMO band gap energy, in this case, was 0.2908 eV. By comparing the results of the TDM in both cases of interaction, it was found that the highest value of TDM belongs to the supposed structure of Term 1SA-3PVA - Mid 1SA. But, the lowest band gap energy obtained is that for 3PVA- (C10) 2SA. Thermal parameters indicted that thermochemical parameters varied according to the PVA/SAcomposite sites.

## 5. REFERENCES


1. Sachan, K.N.; Pushkar, S.; Jha, A.; Bhattcharya, A. Sodium alginate: the wonder polymer for controlled drug delivery. *Journal of Pharmacy Research* **2009**, *2,* 1191-1199.
2. Sun, X.; Chen, J.H.; Su, Z.B.; Huang, Y.H.; Dong X.F. Highly effective removal of Cu(II) by a novel 3-aminopropyltriethoxysilane functionalized polyethyleneimine/sodium alginate porous membrane adsorbent. *Chemical Engineering Journal* **2016**, *290*, 1-11, https://doi.org/10.1016/j.cej.2015.12.106.
3. Wang, Q.; Ju, J.; Tan, Y.; Hao, L.; Ma, Y.; Wu, Y.; Zhang, H.; Xia, Y.; Sui, K. Controlled Synthesis of Sodium Alginate Electrospun Nanofiber Membranes for Multi-occasion Adsorption and Separation of Methylene Blue. *Carbohydr Polym.* **2019**, *205,* 125-134, https://doi.org/10.1016/j.carbpol.2018.10.023.
4. Bidarra, S.J.; Barrias, C.C.; Granja, P.L. Injectable alginate hydrogels for cell delivery in tissue engineering. *Acta Biomater.* **2014**, *10*, 1646-62, https://doi.org/10.1016/j.actbio.2013.12.006.
5. Guiping, M.; Dawei, F.; Liu, Y.; Zhu, X.; Nie, J. Electrospun sodium alginate/poly (ethylene oxide) core–shell nanofibers scaffolds potential for tissue engineering applications. *Carbohydrate Polymers* **2012**, *87*, 737-743, https://doi.org/10.1016/j.carbpol.2011.08.055.
6. Han, Y.; Zeng, Q.; Li, H.; Chang, J. The calcium silicate/alginate composite: preparation and evaluation of its behavior as bioactive injectable hydrogels. *Acta Biomater.* **2013**, *9*, 9107-17, https://doi.org/10.1016/j.actbio.2013.06.022.
7. Remminghorst, U.; Rehm, B.H.A. Bacterial alginates: from biosynthesis to applications. *Biotechnology Letters* **2006**, *28,* 1701-1712, https://doi.org/10.1007/s10529-006-9156-x.
8. Yang, J.S.; Xie, Y.J.; He, W. Research progress on chemical modification of alginate: a review. *Carbohydrate Polymers* **2011**, *84*, 33–39, https://doi.org/10.1016/j.carbpol.2010.11.048.
9. Pawar, S.N.; Edgar, K.J. Alginate derivatization: a review of chemistry, properties and applications. *Biomaterials* **2012**, *33,* 3279–3305, https://doi.org/10.1016/j.biomaterials.2012.01.007.
10. Razzak, M.T.; Darwis, D.; Zainuddin, S. Irradiation of polyvinyl alcohol and polyvinyl pyrrolidone blended hydrogel for wound dressing. *Radiat. Phys. Chem.* **2001**, *62*, 107–113, https://doi.org/10.1016/S0969-806X(01)00427-3.
11. Demerlis, C.C.; Schoneker, D.R. Review of the oral toxicity of polyvinyl alcohol (PVA). *Food Chem. Toxicol.* **2003**, *41,* 319–326, https://doi.org/10.1016/S0278-6915(02)00258-2.
12. Maria, T.M.; Carvalho, R.A.; Sobral, P.J.; Habitantea, A.M.; Solorza-Feriab, J. The effect of the degree of hydrolysis of the PVA and the plasticizer concentration on the color, opacity, and thermal and mechanical properties of films based on PVA and gelatin blends. *J. Food Eng.* **2008**, *87*, 191–199, https://doi.org/10.1016/j.jfoodeng.2007.11.026.
13. Qiu, K.; Netravali, A.N. A Composting Study of Membrane-Like Polyvinyl Alcohol Based Resins and Nanocomposites. *J. Polym. Environ.* **2013**, *21*, 658–674, https://doi.org/10.1007/s10924-013-0584-0.
14. Qiu, K.; Netravali, A.N. Fabrication and characterization of biodegradable composites based on microfibrillated cellulose and polyvinyl alcohol. *Compos. Sci. Technol.* **2012**, *72*, 1588–1594, https://doi.org/10.1016/j.compscitech.2012.06.010.
15. Qiu, K.; Netravali, A.N. Halloysite nanotube reinforced biodegradablenanocomposites using noncrosslinked and malonic acid crosslinked polyvinyl alcohol. *Polym. Compos.* **2013**, *34,* 799–809, https://doi.org/10.1002/pc.22482.
16. Ibrahim, M.; Osman, O. Spectroscopic Analyses of Cellulose: Fourier Transform Infrared and Molecular Modelling Study. *J. Comput. Theor. Nanosci.* **2009**, *6*, 1054–1058, https://doi.org/10.1166/jctn.2009.1143.
17. Ibrahim, M.; Osman, O.; Mahmoud, A.A. Spectroscopic Analyses of Cellulose and Chitosan: FTIR and Modeling Approach. *J. Comput. Theor. Nanosci.* **2011**, *8*, 117-123, https://doi.org/10.1166/jctn.2011.1668.
18. Alghunaim, N. S.; Omar, A.; Elhaes, H.; Ibrahim, M. Effect of ZnO and $TiO_2$On the Reactivity of Some Polymers. *J. Comput. Theor. Nanosci.* **2017**, *14*, 2838–2843, https://doi.org/10.1166/jctn.2017.6583.
19. Ezzat, H.A.; Hegazy, M.A.; Nada N.A.; Ibrahim, M.A. Effect of Nano Metal Oxides on the Electronic Properties of Cellulose, Chitosan and Sodium Alginate. *Biointerface Research in Applied Chemistry* **2019**, *8*, 4143-4149, https://doi.org/10.33263/BRIAC94.143149.
20. Ibrahim, M.; Saleh, N.A.; Elshemey, W.M.; Elsayed, A.A. Hexapeptide Functionality of Cellulose as NS3 Protease Inhibitors. *Medicinal Chemistry* **2012**, *8*, 826-830, https://doi.org/10.2174/157340612802084144.

21. Grenni, P.; Caracciolo, A.B.; Mariani, L.; Cardoni, M.; Riccucci, C.; Elhaes, H.; Ibrahim, M.A. Effectiveness of a new green technology for metal removal from contaminated water. *Microchemical Journal* **2019**, *147*, 1010-1020, https://doi.org/10.1016/j.microc.2019.04.026.
22. Ammar, N.S.; Elhaes, H.; Ibrahim, H.S.; El-hotaby W.; Ibrahim, M.A. A Novel Structure for Removal of Pollutants from Wastewater. *Spectrochimica Acta Part A.* **2014**, *121*, 216-223, https://doi.org/10.1016/j.saa.2013.10.063.
23. Fakhry, A.; Osman, O.; Ezzat H.; Ibrahim, M. Spectroscopic analyses of soil samples outside Nile Delta of Egypt. *Spectrochim. Acta A.* **2016**, *168*, 244–252, https://doi.org/10.1016/j.saa.2016.05.026.
24. Arı, H.; Büyükmumcu, Z. Comparison of DFT functionals for prediction of band gap of conjugated polymers and effect of HF exchange term percentage and basis set on the performance. *Computational Materials Science* **2017**, *138,* 70-76, https://doi.org/10.1016/j.commatsci.2017.06.012.
25. Fahim, A.M.; Shalaby M.A.; Ibrahim, M. Microwave-assisted synthesis of novel 5-aminouracil-based compound with DFT calculations. *J. Mol. Struct*. **2019**, *1194*, 211-226, https://doi.org/10.1016/j.molstruc.2019.04.078.
26. Afzal, M.A.F.; Hachmann, J. Benchmarking DFT approaches for the calculation of polarizability inputs for refractive index predictions in organic polymers. *Phys. Chem. Chem. Phys.* **2019**, *21*, 4452-4460, https://doi.org/10.1039/C8CP05492D.
27. Kleykamp, H. Gibbs Energy of Formation of SiC: A contribution to the Thermodynamic Stability of the Modifications. *Berichte der Bunsengesellschaftfürphysikalische Chemie*. **1998**, 1231–1234, https://doi.org/10.1002/bbpc.19981020928.
28. Stoner, C.D. Inquiries into the Nature of Free Energy and Entropy in Respect to Biochemical Thermodynamics. *Entropy* **2000**, *2,* 106-141, https://doi.org/10.3390/e2030106.
29. Frisch, M.J.; Trucks, G.W.; Schlegel, H.B.; Scuseri, G.E.; Robb, M.A.; Cheeseman, J.R.; Scalmani, G.; Barone, V.; Mennucci Petersson, B.G.A.; Nakatsuji, H.; Caricato, M.; Li, X.; Hratchian, P.H.; Izmaylov, A.F.; Bloino, J.; Zheng, G.; Sonnenberg, J.L.; Hada, M.; Ehara, M.; Toyota, K.; Fukuda, R.; Hasegawa, J.; Ishida, M.; Nakajima, T.; Honda, Y.; Kitao, O.; Nakai, H.; Vreven, T.; Montgomery, J.A.; Jr. Peralta, J.E.; Ogliaro, F.; Bearpark, M.; Heyd, J.J.; Brothers, E.; Kudin, K.N.; Staroverov, V.N.; Keith, T.; Kobayashi, R.; Normand, J.; Raghavachari, K.; Rendell, A.; Burant, J.C.; Iyengar, S.S.; Tomasi, J.; Cossi, M.; Rega, N.; Millam, J.M.; Klene, M.; Knox, J.E.; Cross, J.B.; Bakken, V.; Adamo, C.; Jaramillo, J.; Gomperts, R.; Stratmann, R.E.; Yazyev, O.; Austin, A.J.; Cammi, R.; Pomelli, C.; Ochterski, J.W.; Martin, R.L.; Morokuma, K.; Zakrzewski, V.G.; Voth, G.A.; Salvador, P.; Dannenberg, J.J.; Dapprich, S.; Daniels, A.D.; Farkas, O.; Foresman, J.B.; Ortiz, J.V.; Cioslowski, J.; Fox, D.J. Gaussian, Inc., Gaussian 09, Revision C.01.Wallingford CT, **2010**.
30. Becke, A.D. Density-functional thermochemistry. III. The role of exact exchange. *The Journal of chemical physics* **1993**, *98*, 5648-5652, https://doi.org/10.1063/1.464913.
31. Lee, C.; Yang, W.; Parr, R.G. Development of the ColleSalvetti correlation-energy formula into a functional of the electron density. *Phys. Rev. B.* **1988**, *37*, 785, https://doi.org/10.1103/PhysRevB.37.785.
32. Miehlich, B.; Savin, A.; Stoll, H.; Preuss, H. Results obtained with the correlation energy density functionals of becke and Lee, Yang and Parr. *Chem. Phys. Lett.* **1989**, *157,* 200, https://doi.org/10.1016/0009-2614(89)87234-3.
33. Stewart, J.J.P. SCIGRESS, Version FJ 2.4.x, Fujitsu Limited, United States 2012.
34. Badry, R.; El-Khodary, S.; Elhaes, H.; Nada, N.; Ibrahim, M. The Influence of Moisture on the Electronic Properties of Monomer, Dimer, Trimer and Emeraldine Base Sodium Carboxymethyl Cellulose. *Egyptian Journal of Chemistry* **2019**, *62*, 39-56, https://doi.org/10.33263/LIANBS82.553557.
35. Politzer, P.; Laurence, P.R.; Jayasuriya, K. Molecular electrostatic potentials: an effective tool for the elucidation of biochemical phenomena. *Environ. Health Persp.* **1985**, *61*, 191202, https://doi.org/10.1289/ehp.8561191.
36. Politzer, P.; Murray, J.S. Molecular Electrostatic Potentials: Concepts and Applications. *J. Theor. Comput. Chem.* **1996**, *3*, 649. 27.
37. Şahin, Z.S.; Şenöz, H.I.; Tezcan, H.; Büyükgüngör, O. Synthesis, spectral analysis, structural elucidation and quantum chemical studies of (E)-methyl-4-[(2phenylhydrazono) methyl]benzoate. *Spectrochim. Acta A* **2015**, *143*, 91-100, https://doi.org/10.1016/j.saa.2015.02.032.